Enigmatic ground water enriched in isotopically light lithium

*Yoshiro Nishio[1]

1.Kochi University

Deep crustal fluids may involve with earthquake and volcanic activities. The geophysical survey such as seismic and electrical conductivity tomography can visualize distribution of crustal fluids, while they need abundant fluids for the detection. It is therefore expected that geochemical results provide us detailed information about origin of deep-seated fluids. However, admixture with surface water makes it difficult to draw precise conclusions regarding the origins of deep-seated fluids. Because of this, geochemical results of the deep-seated fluids had been limited. Lithium (Li) is relatively unaffected by surface water contamination because the Li contents of deep-seated fluids are much greater than the surface water content. These high Li concentrations result from dramatically elevated leaching of Li from solid phase into fluids at high temperatures, and the fact that subsequent re-uptake of the leached Li from the fluid by the solid phase (which occurs as the fluid cools) takes a considerable time. In addition, the two stable isotopes of Li are ^{6}Li and ^{7}Li, and their relative abundances are about 7.5% and 92.5%, respectively. Furthermore, the difference in the ^{7}Li/^{6}Li ratio between fluid and solid phases varies with the reaction temperature. As a result, the Li isotope ratio provide us information about origin of deep-seated fluids. Based on the Li isotopic results on ground water samples, we have researched the origin of deep-rooted fluids. One of major problems unsolved is that significantly low ^{7}Li/^{6}Li ratios are observed in several ground water samples. The Li isotope composition of fluid phase is currently heavier than that of solid phase. Therefore, the significantly low ^{7}Li/^{6}Li ratios of ground waters require the solid phase other than the crust or mantle. Nishio et al. (2010) reported that the significantly low ^{7}Li/^{6}Li ratios were observed in the southeast flank of Ontake volcano in central Japan. Since 1976, earthquake swarms have occurred beneath the southeast flank of Ontake volcano. Electrical conductivity surveys have shown that these earthquake swarms are associated with the upwelling of deep-seated fluid. Based on the Li and Sr isotopic results of ground water samples around Ontake volcano, Nishio et al. (2010) concluded that the fluid associated with the earthquake swarms beneath the southeast flank of Ontake volcano is not a simple volcanic fluid. However, it is still unknown the origin of significantly low ^{7}Li/^{6}Li ratios. Afterwards, such significantly low ^{7}Li/^{6}Li ratios were observed in ground water samples in the Kobe and Kochi area (unpublished data). Accordingly, I’ll discuss about the origin of the significantly low ^{7}Li/^{6}Li ratios observed in several ground water samples.

Reference:

Nishio et al., 2010. Lithium and strontium isotopic systematics of waters around Ontake volcano, Japan: Implications for deep-seated fluids and earthquake swarms. Earth Planet. Sci. Lett. 297, 567-576.

Keywords: lithium isotope, deep crustal fluid, slab-derived fluid, geochemical thermometer

Relationships between crustal stress fields and geological structures on pathways of upwelling deep-seated water at Kii Peninsula, southwest Japan

*Makoto Otsubo[1], Tooru Shimizu[1], Ayumu Miyakawa[1], Tsutomu Sato[1], Michiko Ohwada[1], Kohei Kazahaya[1]

1.Geological Survey of Japan/AIST

The natural and hot springs with $^3He/^4He$ ratios higher than the atmospheric values are recognized to occur in nonvolcanic regions on the Kii Peninsula in the forearc regions of southwestern Japan arc (Sano & Wakita, 1985; Wakita et al., 1987; Matsumoto et al., 2003; Umeda et al., 2006, 2007), indicating that there are upwelling paths of the mantle-derived fluids in this region. A number of deep groundwater and natural spring water in this region are found to contain the slab-derived deep-seated fluid component, whose isotopic composition is similar to magmatic with the high Li/Cl ratio (>0.001 in wt. ratio) (Kazahaya et al., 2014). The upwelling of the deep-seated water provides significant information to understand the fluid movement in the crust and the water cycle in the subduction system (e.g. Hacker, 2008).
In this study, we present the upwelling of water and gas along the fractures and the relationships between orientations of the veins and the upwelling of the deep-seated water in the Shiotakibashi outcrop located to the north of Median Tectonic Line (MTL). And, we discuss the upwelling process of the deep-seated water at Kii Peninsula by using the relationships between crustal stress field and geological structures.
The Shiotakibashi outcrop along the Ishikawa river at the Kawachinagano city of Osaka prefecture is one of regions where the upwelling of the water and gas containing deep-seated water along the fractures can be observed (Tanaka et al., 2013). In the upwelling points at the outcrop, the patches of fractures that cut the Cretaceous granite belonging to the inner zone are filled by the calcite crystalized from the water. Furthermore, the water and gas are flowing so as to avoid the filled fractures. And, we can observe many mineral veins with several orientations in this outcrop. Mineral veins can provide evidences of the ancient fluid migration along the fractures.
In this study, we measured the strike, dip and width of the veins in a single outcrop of the Shiotakibashi outcrop (~100 veins). On the veins, the fractures that cut the cretaceous granite are filled by the calcite. The veins have thicknesses with a few mm to 2 cm. The most of the veins have NNE-SSW and ENE-WSW striking and dip with high angle while some veins have horizontal dip. The dilation tendency (Ferrill et al., 1999) for the filled fractures in the present stress inferred from the major active faults in the eastern part of the southwestern Japan including the Kii Peninsula (Tsutsumi et al., 2012) indicate that the fractures with upwelling of water and gas have high tendency on the pass ways of deep-seated water. Hence, the present tectonic stress may be feasible for upwelling of the deep-seated water along the fractures for a part of the fractures.
At the map scale, the Cretaceous-Paleogene accretionary complex, Shimanto Belt is exposed in the region located to the south of MTL in Kii Peninsula. The most of deformation structures of the Shimanto Belt have northward plunging thrusts. Based on the relationships between crustal stress field and attitudes of the geological structures, the dilation tendency is high on the geological structures. Hence, we suggest that the geological structures of the region under the present crustal stress are favorable pathways for deep-seated fluids.

Keywords: stress, fluid migration, fault, crust, deep low-frequency tremors, subduction zone

Three dimensional attenuation structure beneath the northwestern part of Kii peninsula, central Japan

*Noriko Tsumura[1], Naoki Mizuno[2], Eri Umeyama[1], Aitaro Kato[3], Eiji Kurashimo[4], Takashi Iidaka[4], Shin'ichi Sakai[4], Atsushi Saiga[5]

1.Graduate School of Science, Chiba University, 2.Faculty of Science, Chiba University, 3.Graduate School of Environmental Studies, Nagoya University, 4.Earthquake Research Institute, University of Tokyo, 5.JAEA

Beneath the Kii peninsula which is located above the subducting Philippine Sea (PHS) plate, it is known that there are several interesting seismic phenomena such as an intensive seismic swarm in the shallow crust and occurrence of non-volcanic low frequency earthquakes around the top of the PHS plate at the depths between 30-40km [Mizoue et al.,1983; Kato et al.,2010]. Previous geophysical studies suggested that geofluid is related to the occurrence of such seismic events [Hirose et al.,2008; Kato et al.,2010&2014]. In this study, we determined a 3-dimensinal attenuation structure to obtain a new information about physical properties in the study region because Q value is a sensitive parameter for the existence of fluid or cracks and effect of temperature.

We applied a combined inversion in which source parameters, site effects and Q values are determined simultaneously [Tsumura et al.,2000] for small earthquakes' spectra. Seismic waveforms were observed at the routine Hi-net seismic stations by NIED and temporary dense seismic arrays of arranging east-west direction and north-south direction at the southern and western parts of the Kii peninsula, respectively. We selected 247 earthquakes which were recorded at 113 seismic stations and calculated 8616 spectra for P arrivals of time window 1.28s for taking into account ray distribution.

Derived Qp images show that high attenuation zone(Qp<200) exists at the northwestern part of Kii peninsula in the depths shallower than 15km. This high attenuation zone has the similar horizontal extent as that of seismic swarm's source region. The other region shows moderate Qp(about 400 to 800) except the southern part of the Kii peninsula where Qp is less than 400. For the depths between 15 to 38km, high attenuation zone continued from the shallower part beneath the swarm region, however its horizontal extent becomes small at the deeper than 25km. We found that patch-like high Qp zones were distributed in the region just above isodepth contour 30 to 40km of the PHS plate. These high Qp regions coincide with the region where many low frequency earthquakes occur. In the NW-SE vertical Q cross section at the western part of the Kii peninsula, we can clearly see that the high attenuation zone is located just beneath the seismic swarm region and its distribution corresponds to a low velocity zone estimated from travel time tomography [Hirose et al.,2008; Kato et al.,2014]. From the result of reciever function analysis[Kato et al.,2014] , subducting Philippine sea plate's oceanic basalt is considered to start conversion to eclogite just beneath the swarm region and the high attenuation and low velocity zone may reflect the existence of fluid due to the dehydration proceess. Another feature we should mention is existence of low attenuation zone at the mantle wedge just above the source region of low frequency earthquakes. This low attenuation zone shows higher velocity than surroundings. We'd like to integrate various geophysical data and argue the physical property of these regions.

[References]Hirose et al., J. Geophys. Res., 113, B09315, doi:10.1029/2007JB005274;Kato et al., Geophys. Res. Lett., 37, L15302, doi:10.1029/2010GL043887;Kato et al., EPS, 66:18,2014;Mizoue et al., Bull. Earth Res. Inst., 58,287-310,1983;Tsumura et al., Tectonophysics, 319, 241-260, 2000

Keywords: Q attenuation, seismic swarm, non-volcanic low frequency earthquake, Kii peninsula, southwest Japan

Control of episodic tremor and slip by high-pressurized fluids: a new constraint from ScSp waves

*Mitsuhiro Toya[1], Aitaro Kato[1], Takuto Maeda[2], Kazushige Obara[2], Tetsuya Takeda[3], Koshun Yamaoka[1]

1.Graduate School of Environmental Studies, Nagoya University, 2.Earthquake Research Institute, the University of Tokyo, 3.National Research Institute for Earth Science and Disaster Prevention

1. Introduction

High-pressurized fluids are thought to play an important role in controlling episodic tremor and slow slip (ETS) in subduction zones [e.g., Shelly et al., 2006; Audet et al., 2009]. Therefore, constraining the along-dip distribution of ETS is necessary to better understand its source mechanism, and particularly the role played by fluids in ETS generation. Here, we report clear observations of coherent *ScSp* phases with a dense seismic array in western Shikoku, Japan. To reproduce these observations, we performed numerical simulations of elastic-wave propagation using a finite difference method (FDM) that incorporated a three-dimensional structural model. The combination of coherent *ScSp* phases and numerical simulations allows us to investigate the depth dependence of Poisson’s ratios within the LVZ, and to quantitatively estimate local changes in fluid pressure in the ETS zone.

2. Data and Method

We deployed a dense linear seismic array from October 2011 to April 2013 on western Shikoku Island, SW Japan. We also used permanent stations near the array from the Hi-net network, operated by the National Research Institute for Earth Science and Disaster Prevention [Okada et al., 2004], and stations of the Japan Meteorological Agency. During the deployment period, we visually inspected seismograms of Mw ≥6 deep earthquakes with focal depths greater than 90 km and epicentral distances D < 25°. Using the transverse components of rotated seismograms from the array, we shifted the *ScS* phases relative to the arrival at the station having the highest S/N ratio by cross-correlating the *ScS* phase from the station with other *ScS* waveforms to achieve the maximum correlations. The vertical component data at each station were then time shifted by the corresponding time lags, relative to the station.

3. Results and Discussion

Based on comparisons of transverse and vertical component waveform data, we found clear, coherent signals arriving before *ScS* on the vertical components of most stations in the array. The travel time differences between *ScS* and *ScSp* increase along the direction of subduction. This means that the *ScS-to-ScSp* conversion point deepens to the northwest, indicating in turn that the converted waveforms propagate from the top of the subducting PHS Plate. Then, we simulated the propagation of synthetic *ScSp* waveforms using the JIVSM model [Koketsu et al., 2012]. However, the calculated *ScS* -*ScSp* travel time differences were systematically smaller than predicted by our observations. To improve the goodness of fit, we partitioned the LVZ into shallower and deeper parts around the upper corner of the mantle wedge, because the travel time difference between the observed and simulated waveforms was larger at the northern stations, toward which the LVZ is subducting. This change gave two different *S*-wave velocities in the LVZ. We conducted a grid search over the three-parameter space defined by two velocities, and the layer thickness *h* of the LVZ. To quantify the fit, we averaged the cross-correlation coefficients between observed and simulated *ScSp* phases. From the grid search results, the Vp/Vs ratio must be higher beneath the mantle wedge corner than at shallow depths, regardless of the assumed LVZ thickness. In the best model, Vp/Vs ratios within the subducting oceanic crust increase by 0.3 beneath the mantle wedge corner, where ETS has been observed. This high-Vp/Vs layer indicates the presence of high-pressurized fluids confined at ETS source depths. Based on extrapolation of laboratory measurements [Peacock et al., 2011], we infer that the observed changes in Vp/Vs ratios correspond to an increase in fluid pressure of ~20 MPa relative to the updip, locked zone (Figure 1).

Keywords: episodic tremor and slow slip, ScSp phase, high-pressurized fluid

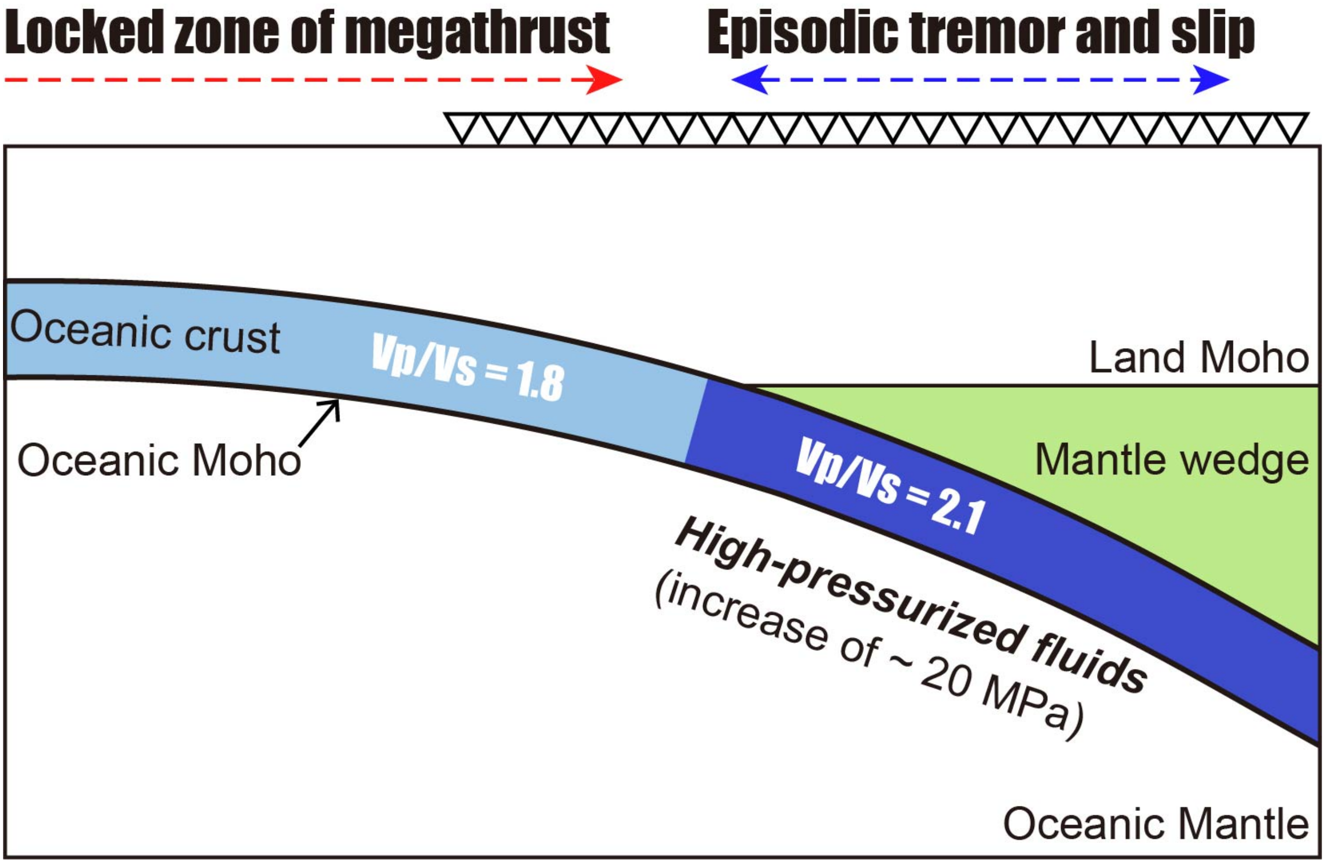

Dynamics of rock fracture permeability explored through MEQs

*Takuya Ishibashi[1], Noriaki Watanabe[2], Atsushi Okamoto[2], Nobuo Hirano[2], Hiroshi Asanuma[1], Noriyoshi Tsuchiya[2]

1.Fukushima Renewable Energy Institute, AIST, 2.Graduate School of Environmental Studies, Tohoku University

For the success of unconventional geothermal reservoirs (i.e. EGS), maintaining conduits with high-fluid-throughput is desirable. Hydraulic stimulation for such reservoirs is recognized as one of the most general ways to improve or maintain their crustal permeability, which is known as the key parameter controlling crustal fluid flow [*Ingebristen and Manning*, 2010]. During the hydraulic stimulation, in-situ microearthquakes (MEQs) data are basically recorded to capture the underlying active processes and the permeability evolution within the reservoir [*Majer et al.*, 2007], and these MEQs are in general regarded as signals that somehow represent permeability change in a fractured reservoir. If we have an insight into quantitative linkage between the permeability change and MEQ, such an insight is definitely useful for mapping in-situ permeability evolution in a reservoir. However, it remains ambiguous how much the fracture permeability is enhanced by a MEQ.

In the present study, we explore a linkage between fracture permeability change and MEQs. For this purpose, we first prepared heterogeneous aperture distributions for rock fractures with various combination of fracture length (m), l, and shear displacement (m), d, according to the method of *Ishibashi et al* [2015]. Through the analyses of these aperture distributions, scale dependencies of fluid flows through joints, i.e. fractures without shear displacement, and faults, i.e. fractures with shear displacement of d (m), are predicted as followings. Both joint and fault aperture distributions are characterized by a scale-dependent geometric mean and a scale-independent geometric standard deviation of aperture. Changes in the geometric means of joint and fault apertures (mm), $e_{m,\ joint}$ and $e_{m,\ fault}$, with fracture length (m), l, are approximated by $e_{m,\ joint} = 1.3\times10^{-1} l^{0.10}$ and $e_{m,\ fault} = 1.3\times10(d / l)^{0.59} l^{0.71}$, whereas the geometric standard deviations of both joint and fault apertures are approximately 3. Fluid flows through both joints and faults are characterized by formations of preferential flow paths (i.e., channeling flows) with scale-independent flow areas of approximately 10%, whereas the joint and fault permeabilities (m^2), k_{joint} and k_{fault}, are scale dependent and are approximated as $k_{joint} = 9.8\times10^{-13} l^{0.16}$ and $k_{fault} = 2.3\times10^{-6}(d / l)^{1.18} l^{1.08}$. By coupling these scaling laws with the concept of moment magnitude [*Hanks and Kanamori*, 1979], quantitative change in mean aperture ($e_{m,\ fault}/e_{m,\ joint}$) and fracture permeability (k_{fault}/k_{joint}) are successfully linked with moment magnitude of MEQs (M_w) during hydraulic stimulation for a reservoir as $e_{m,\ fault}/e_{m,\ joint} = 1.0\times10^{0.35Mw}$ and $k_{fault}/k_{joint} = 116.4\times10^{0.46Mw}$. Validity of the equation will be discussed through comparisons with some data of real field development/experiments (e.g., EGS system in Basel and Soultz-sous-Fôret).

In summary, such linkages may enable rough inverse-mapping of evolving fracture permeabilities using in-situ MEQ data. This mapping will facilitate new insights into transport phenomenon within the Earth’s crust and it relevant to engineering and scientific applications such as the development of geothermal or hydrocarbon reservoirs and clarification of earthquake mechanisms.

Keywords: rock fracture, permeability, surface topography, microearthquake

Bidirectional replacement zoning developed in metasomatic reaction of olivine and its implication for development of mesh zoning of serpentinites

*Ryosuke Oyanagi[1], Atsushi Okamoto[1], Noriyoshi Tsuchiya[1]

1.graduate school of environmental studies, tohoku university

Serpentnization reaction, which occur though a coupled process of mass transfer, surface reaction, and volumetric expansion, affects both chemical and physical properties of oceanic lithosphere. Mesh texture characterizes most serpentinized peridotite. Mesh rims are considered to be formed via precipitation from a fluid bringing Mg, Fe, and Si into the rock from external resources (e.g., Andreani, 2004, 2007), or replacement reaction after/before mesh core formation (e.g., Beard et al., 2009; Schwarzenbach et al., 2016); However, it is difficult to interpret the processes of mesh texture development and related volumetric changes and mass transfer from texture.
In this study, we conducted hydrothermal experiments using mineral powder of plagioclase and olivine, and found Al-rich serpentine (Al-serpentine) which has a characteristic chemical zoning was formed around contacts between olivine and plagioclase via metasomatic reaction of Si and Al, while lizardite + brucite + magnetite was formed at far from the boundary. Al content in Al-serpentine once decreases from core to rim, and increases. At the center of chemical zoning which has relative low Al content, and a clear outline is observed in its texture. It could be interpreted that the outline preserves an outline of pre-existed olivine, therefore it suggests reaction front propagated both inside and outside direction of olivine. The chemical zoning was formed due to changes of Si and Al concentration in reacting fluid which may occur via metasomatic reaction front propagation. Hydration reaction proceeds toward inside direction requires removal Mg, Fe, and Si to fluid on serpentinization. The removed components from olivine and Si and Al from plagioclase were transported to pore and precipitated at outside.
This experiment used mineral powder (25-53μm) and initial porosity is ~40%; therefore, our experimental results represent an analogue of serpentinization in natural hydrothermal systems with a high porosity such as serpentinization of highly fractured peridotite. It is usually considered that mesh core and rim were formed in another stage. Our result showed a large mass transfer were required on iso-volumetric serpentinization which proceeds toward inside, and reaction towards inside proceeds to make mesh core and reaction towards outside proceeds to make mesh rim, simultaneously; therefore, mesh rim and core could be formed in same stage. On that, the thickness of mesh core represents the thickness of olivine that has been replaced while mesh rim was enlarged with volumetric expansion.

Keywords: serpentinization, mass transfer, mineral replacement, metasomatism, hydrothermal experiment

Seismic velocity and seismicity in the subducting crust of the Pacific slab beneath the eastern part of Hokkaido

*Takahiro Shiina[1], Junichi Nakajima[2], Toru Matsuzawa[1], Genti Toyokuni[1], Saeko Kita[3]

1.Research Center for Prediction of Earthquakes and Volcanic Eruptions, Graduate School of Science, Tohoku University, 2.Graduate School of Science and Engineering, Tokyo Institute of Technology, 3.Graduate School of Science, Hiroshima University

Fluid in subduction zones is considered to play important roles for genesis of intermediate-depth earthquakes (e.g., Kirby et al., 1996) and arc magmatism (e.g., Nakajima et al., 2013). The subducting crust located at the uppermost part of the oceanic plate involves a large amount of water in form of hydrous minerals, and released fluid by dehydration reaction of the hydrous minerals lowers seismic velocity (Hacker et al., 2003). Therefore, it is important to reveal the detailed seismic velocity structure in the subducting crust to understand seismogenesis and water circulation in the subduction zones.
At the western side of the Hidaka mountain range, distinct later phases are often observed for intermediate-depth earthquakes in the Pacific slab (e.g., Shimizu and Maeda, 1980; Abers, 2005). The later phases that are recorded for earthquakes occurred near the upper boundary of the Pacific slab are interpreted as guided waves propagating in the subducting crust (Shiina et al., 2014).
In this study, we estimated P- and S-wave velocities in the subducting crust beneath the eastern part of the Hokkaido by using travel times of the guided waves. The number of earthquakes that guided-P and the guided-S waves were identified in this study were 315 and 275, respectively. Then, we obtained P-wave velocity of 6.5-7.5 km/s, S-wave velocity of 3.6-4.2 km/s, and Vp/Vs of 1.80 at depths of 50-100 km. The P- and S-wave velocities at depths shallower than 80 km are lower than those expected for the fully-hydrated MORB (e.g., Hacker et al., 2003), and the low-velocity anomalies can be explained by the existence of 1 vol% of aqueous fluid.
The P-wave velocity obtained at depths of <80 km beneath the eastern Hokkaido is coincident with that observed in Tohoku (Shiina et al., 2013), while the P-wave velocity at depths of 80-100 km are faster than that estimated in Tohoku district. It is expected that temperatures around the upper boundary of the Pacific slab beneath the eastern Hokkaido are higher than beneath Tohoku, as a result of an oblique subduction of the Pacific slab (e.g., Kita et al., 2010; Abers et al., 2013; Wada et al., 2015). High temperatures beneath eastern Hokkaido may affect location of dehydration reactions of hydrous minerals and fluid migration paths from the subducting crust to the mantle wedge. Therefore, the differences in P-wave velocities between the eastern part of Hokkaido and Tohoku at depths of 80-100 km may be caused by the differences in the amount of fluids trapped in the crust.

Keywords: Subducting crust, Seismic velocity, Guided wave, Upper plane seismic belt

Three-dimensional numerical modeling for subduction thermal regime, slab dehydration, and mantle flow beneath Kanto to Tohoku, Japan

*Yingfeng Ji[1], Shoichi Yoshioka[1]

1.Research Center for Urban Safety and Security, Kobe University

To better understand thermal regimes of the interplate and slab-slab contact zone undergoing subduction upon convergence such as in Kanto to Tohoku, Japan, we developed a parallelepiped three-dimensional thermal convection model to simulate simultaneous subduction of the overlapped Philippine Sea and the Pacific plates. We investigated the interactive slab thermal regime and mantle flow associated with such a unique geodynamic process, using simplified and realistic models. Results showed that: (1) cold anomaly was found to exist predominantly on the slab contact zone, resulting in a cold triple-plate junction corner immediately above the zone with an estimated temperature colder by approximately ~300°C beneath Kanto than Tohoku. As a result, delay in slab dehydration takes place and accounts for the distribution of low seismic velocities in the slab contact zone; (2) a relative subduction direction that yields the obliquity or asymmetry of the thermal structure in the slab contact zone, which corresponds to thermally controlled clustered seismicity on the southwestern half of the slab contact zone probably due to the delayed slab dehydration; (3) induced flow in the continental mantle was related to the straight component of subduction velocity of the lower oceanic plate more than to slab thickness. Interaction between the two oceanic plates determined the induced poloidal and toroidal convections in the continental mantle. In the sandwiched mantle wedge, the mantle flow induced by the Pacific plate is predominant, and reaches depths of 30~100 km beneath Kanto, which is shallower than Tohoku, and attributable to the double subduction; (4) thermal regime and dehydration of MORB near the upper surface of the subducted Pacific plate is considered to control distribution of seismicity beneath Tohoku and Kanto.

Keywords: slab dehydration, dual subduction, numerical simulation, thermal regime

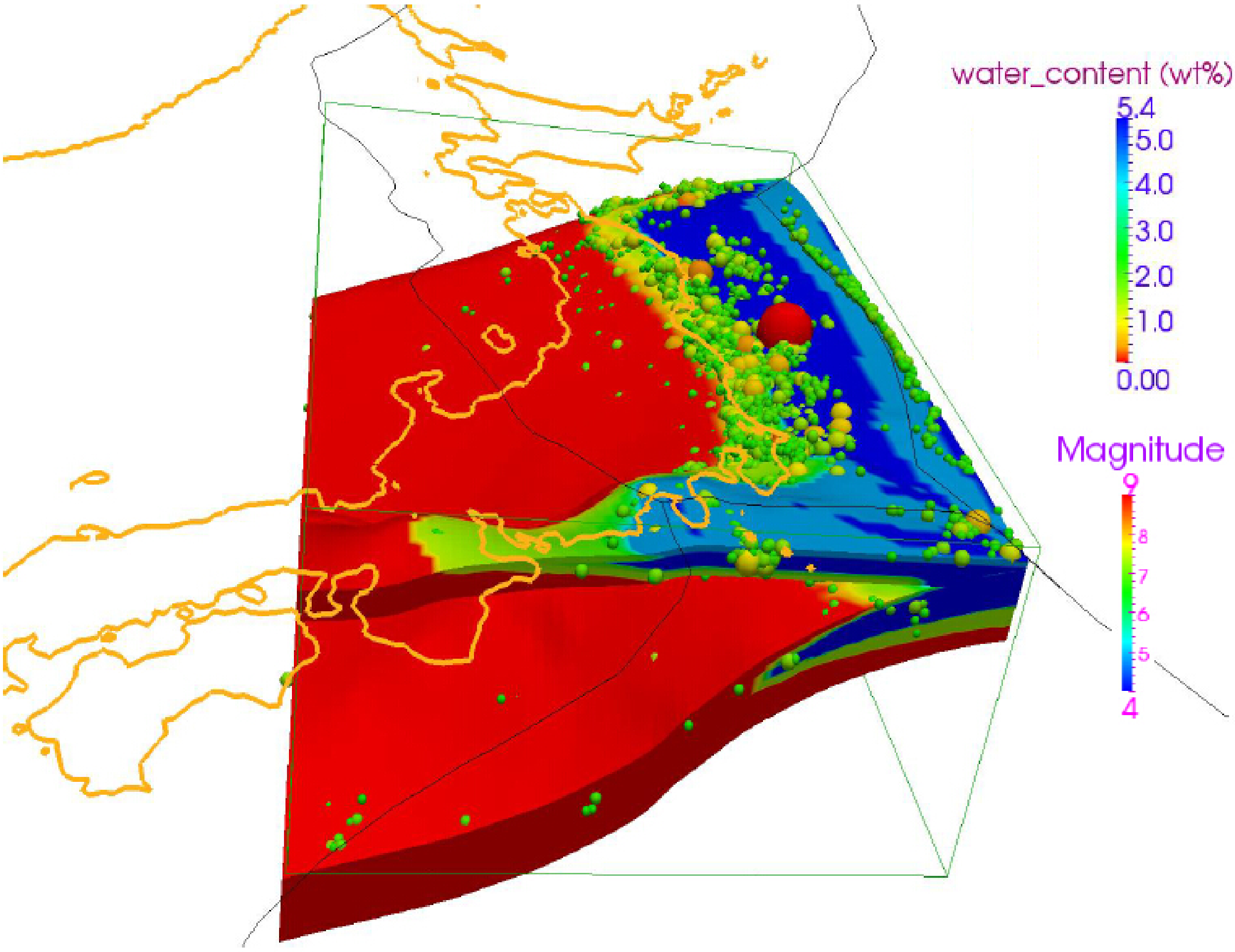
water_content (wt%)
5.4
5.0
4.0
3.0
2.0
1.0
0.00
Magnitude
9
8
7
6
5
4

Geo-fluids distribution in mantle inferred from the electrical conductivity and simulated thermal structures beneath Kyushu

*Maki Hata[1], Makoto Uyeshima[2], Shoichi Yoshioka[3]

1.Advanced Industrial Science and Technology, 2.Earthquake Research Institute, The University of Tokyo, 3.Research Center for Urban Safety and Security, Kobe University

The Kyushu Island, at which the oceanic Philippine Sea Plate subducts into the mantle beneath the continental Eurasia Plate, is characterized by the northern and southern volcanic regions and the central non-volcanic region. Magmatism in the subduction zones is triggered by the addition of the oceanic slab-derived aqueous fluids (water) to the mantle, because solidus of the mantle rock falls by the addition of the aqueous fluids and partial melting of the mantle occurs. Thus the determination of geo-fluids (the aqueous fluids and the melts) distribution is essential to understand the magmatism in the Kyushu subduction zone including the non-volcanic region between the two volcanic regions.
We obtained an electrical conductivity structure (model) beneath the entire Kyushu Island using three-dimensional inversion analyses and found three conductive anomalies, which indicate the different intensity and spatial extent for the three regions, at the mantle in the model [Hata et al., 2015]. The difference is considered to originate in the content of geo-fluids in the mantle. We determined the temperature and melt fraction distributions (structures), as a function of a fixed water content, inferred from the electrical conductivity structure beneath the Kyushu Island by using petrological laboratory-derived results [Hata and Uyeshima, 2015]. The laboratory-derived results are the relation between electrical conductivity and temperature for four nominally anhydrous minerals (Olivine, Orthopyroxene, Clinopyroxene, and Garnet) and hydrous basaltic melt in solid and liquid phases of the mantle, and the relation between melt fraction and temperature for mantle rocks (peridotites) under a condition of isobaric hydrous mantle melting.
In this study, we aim to determine the content of both geo-fluids in the mantle beneath the Kyushu Island. Thus we use a fixed thermal structure, which is a simulated thermal model associated with the subduction of the Philippine Sea Plate [e.g., Yoshioka et al, 2008]. Then we determine the geo-fluids distribution by integrating the simulated thermal structure of the mantle, field-derived electrical conductivity structure of the mantle, and laboratory-derived electrical conductivity of the four mantle minerals and the basaltic melt. We will describe our approach to determine the content of the geo-fluids and show the water content distribution and the melt fraction distribution in the mantle beneath the Kyushu Island.

Dynamics of heat and material transportation during subduction initiation in the Setouchi Volcanic Belt

*Fumitoshi Morisato[1], Tsuyoshi Iizuka[1], Hirochika Sumino[2], Tomoyuki Shibata[3], Masako Yoshikawa[3], Kazuhito Ozawa[1]

1.Department of Earth and Planetary Science, Graduate School of Science, The University of Tokyo,
2.Department of Basic Science, Graduate School of Arts and Sciences, The University of Tokyo,
3.Beppu Geothermal Research Laboratory, Kyoto University

Kowledge of subduction initiation is critical for better understanding dynamics of plate tectonics, but is difficult to obtain because of its episodic and transient nature resulting in incomplete and fragmental records. The key issue is elucidation of heat and material transportation in a subduction zone during the subduction initiation. The aim of this study is clarify spatial and temporal changes of thermal state and material distribution involved in volcanisms of the Setouchi Volcanic Belt to scrutinize subduction initiation by exploiting its excellent records of the processes of subduction initiation.

The Setouchi Volcanic Belt (SVB) in the Southwest Japan arc has a record of igneous activities which show temporally and spatially continuous distributions in the forearc region in the Miocene period. The SVB is characterized by the occurrence of primitive volcanic rocks such as high-Mg andesite (HMA) and basalt. Previous studies in the Shodoshima Island and Osaka argued that HMA magmas are generated by highly wet melting of the wedge mantle involving slab melt from the subducting young and hot Shikoku Basin in the early stage of subduction initiation (Furukawa & Tatsumi, 1999; Shimoda & Tatsumi, 1999; Tatsumi et al., 2006). However, there are several issues that must be addressed: (1) HMAs are very poor in water; (2) the estimated melting conditions for HMA and basaltic magmas are very disparate: hydrous and 1050 to 1150 ℃ vs. less hydrous and 1300 ℃, which are supposed to have been close in time and space in the mantle; and (3) the proposed magma genesis is highly dependent on data in a particular and restricted domain (< 20 km in width) in spite of the wide extension of SVB (600 km in width) consisting of several domains with higher concentration of volcanisms.

There are three sectors of higher frequency of volcanic rock distribution in the SVB on the scale of about 100km scale, each of which may correspond to a separated domain of magma generation. We selected north-eastern part of the Shikoku (NE Shikoku), as study area, where magma genesis has not scrutinized yet. We measured whole rock composition of lavas by using XRF, LA-ICP-MS, and ICP-MS and mineral chemical compositions of phenocrysts with EPMA, and obtained K-Ar ages for samples collected from this sector in the SVB.

Our estimation of a primary magma for HMAs in the north-eastern Shikoku, which is based not only on whole rock major element compositions but also on chemical zoning of phenocrysts, is more magnesian (> 11.6 wt% MgO) than that of the previous study. Geothermometer of Sugawara (2000) combined with liquidus drop after Méderd & Grove (2008) and alpha MELTS program (Ghiorso et al., 2001; Asimow et al., 2003) constrains melting condition of the primary magma as 1GPa and 1200-1240 ℃ with 1.5-0.9 wt % H2O. The pressure and temperature are close to the basaltic magma generating conditions proposed by Tatsumi (1982). Because of the similarity of major element compositions, the generation conditions of the HMA magma could be common throughout the SVB. By contrast, the whole rock trace element compositions and K-Ar ages show spatial and temporal variations, which suggest variability in timing and extent of supply of a slab-derived component (marked by high LILE/HREE) and/or an enriched mantle component (marked by high HREE abundance). There is a tendency that these components were added in a later stage in a given area.

We argue that achievement of temperature over 1200℃ just beneath the crust for generation of HMA and basalt magmas with temporal changes of source material and involvement of slab-derived fluid components were caused by several local mantle upwellings. Such upwelling induced by the subduction initiation might have entrained slab and/or enriched source components at the leading edge of subducting slab.

Keywords: subduction initiation, high-Mg andesite, The Setouchi Volcanic Belt

Deformation and metasomatic histories of Pinatubo peridotite estimated from microstructural observation

*Takafumi Yamamoto[1], Jun-ichi Ando[1], Naotaka Tomioka[2], Tetsuo Kobayashi[3]

1.Department of Earth and Planetary Systems Science, Hiroshima University, 2.Kochi Institute for Core Sample Research, Japan Agency for Marine-Earth Science and Technology, 3.Department of Earth and Environmental Science, Kagoshima University

Deformation microstructures of olivine in naturally deformed peridotites are useful for examining the rheological properties and deformation history in the upper mantle. Particularly, slip system of deformed olivine is especially well known as an indicator for the deformation conditions, such as temperature, stress, pressure or water content. Here, we try to estimate the deformation history of deformed peridotite by means of the microstructural observation and slip system determination. Two types of amphibole-bearing harzburgite samples (namely P-3 and P-4) collected from Pinatubo volcano were analyzed using optical microscope, SEM, EBSD, TEM and STEM. Kawamoto et al. (2013) suggests that these peridotites were affected by the intense metasomatism. We report the relationship between the deformation history and metasomatic reaction.
Pinatubo peridotites are composed of relatively coarse olivine grains with several mm in size, and partly fine orthopyroxene and amphibole aggregate with tens to hundreds μm in size. The fine grained aggregate in P-4 is more than in P-3. The grain boundaries of the coarse grains exhibit irregular shapes. And these grains show the undulose extinction and well-developed subgrain boundaries. The coarse olivine grains contain a lot of fluid inclusions. Additionally, the fine olivine grains exist along the secondary inclusions within some coarse olivine grains.
The LPO patterns of the coarse olivine grains in the both samples imply the dominant activation of [100]{0kl} slip system, which is developed under high temperature, low pressure and dry deformation conditions. On the other hand, the dominant slip systems obtained from the direct characterization of dislocations by TEM are [100](001), [001](010) or [001](100), which activate under moderate to high water content condition. The discrepancy of the obtained slip systems is probably caused by the overprinting due to the changing of deformation conditions. Dislocation microstructures are more easily modified by later deformation events than LPOs.
We conclude from the characterization of microstructures in combined with the result of Kawamoto et al. (2013) that Pinatubo peridotite experienced deformation and metasomatic events in the following manner. Pinatubo peridotites have originally deformed under high temperature, low pressure and dry conditions in the back-arc region. Then, they have moved to the fore-arc region due to the corner flow, and have been affected by the fluid-related metasomatism. Finally, they have undergone the annealing process within the upwelling magma.
Referenece: Kawamoto et al. (2013) PNAS, 110, 9663.

Keywords: Olivine, Deformation, Metasomatism, Slip system

Dynamics of back-arc spreading

*Kazuhiko Ishii[1], Hirotsugu Nodake[1]

1.Department of Physical Science, Graduate School of Sciences, Osaka Prefecture University

To understand the dynamics of back-arc spreading, we perform 2D numerical simulations. This model is 1200 km depth and 4000 km width and is composed of continental crust, oceanic crust, upper mantle, mantle transition zone and lower mantle. Each rock types have a visco-plastic rheology prescribed by the temperature and pressure dependent linear viscosity, the effective frictional coefficient and the maximum yield stress. We focused on the effects of three parameters, the slab strength (the maximum yield stress), the Clapeyron slope of the 410 km phase transition and the strength of boundary between subducting and overriding plates (the effective frictional coefficient of the oceanic crust).
Most results show periodic change in slab geometry and back-arc spreading rate and their period changes with the parameters. The result for a low maximum yield stress (200 MPa) shows tightly folded slab geometry. The result for a high maximum yield stress (800 MPa) shows relatively flat slab geometry and continuous back-arc spreading. As geological observations show that most back-arc basins formed by 10-20 Myr spreading and the tightly folded slab has not been reported by seismic tomography, we think that the result for a moderate maximum yield stress (500 MPa) reproduce the processes in subduction zones well. We compare the results of simulations with the slab geometry and the history of back-arc spreading in the Izu-Bonin-Mariana subduction zone, and discuss the condition for the start and end of back-arc spreading.

Keywords: subduction zones, slab-mantle interaction, numerical model

What control the position of volcanic arc?

*Kazuhiko Ishii[1]

1.Department of Physical Science, Graduate School of Sciences, Osaka Prefecture University

To understand physical and chemical processes in subduction zones, I use 2D numerical model that include the dehydration of subducting slab, hydration of mantle wedge, water fluxed melting of mantle wedge, change in peridotite composition through melt extraction and addition, solid flow of mantle wedge with temperature, pressure, stress and water content dependent rheology and migration of aqueous fluid and melt through permeable flow. I present the calculation results for five subduction zones that span normal ranges in subducting slab age, convergence velocity, and slab dip angle. The model shows the following general features. A hydrous layer saturated with water in NAMs and rich in aqueous fluid is developed just above the subducting slab surface due to the dehydration of the slab. This layer consists of harzburgite formed by the melt extraction from lehrzolite. The high solidus temperature of the harzburgite suppresses melting of the mantle wedge just above the slab surface and results in melt distribution nearly parallel to and separated at some distance from the subducting slab surface. The depth for slab dehydration and the melt distribution in mantle wedge show general agreement with the seismological observations. The comparison between the results of present model and the geophysical and geological observations indicates variable melting mode for the formation of volcanic front: the flux melting caused by the dehydration of oceanic crust for NE Japan and N Chile, the flux melting caused by the dehydration of mostly slab mantle for Nicaragua and Bonin, and slab melting (slab-melt flux mantle melting) for SW Japan. This variation may be a cause for the wide range of depth to the slab surface below the volcanic front.

Keywords: Subduction zones, Numerical model

Along-arc variation in the slab-mantle coupling due to a thin, low viscosity layer just above the slab

*Manabu Morishige[1]

1.Institute for Geothermal Sciences, Graduate School of Science, Kyoto University

In order to understand how seismic and volcanic activities occur in the subduction zone, it is critical to better understand the thermal structure there. Previous studies have shown that many factors affect the thermal structure including slab velocity, plate age, temperature dependence of viscosity, viscous anisotropy, complex slab geometry, and slab-mantle coupling. Among these factors, I focus on slab-mantle coupling in this presentation. It is well known mainly based on the observed low surface heat flow and low seismic attenuation that the forearc mantle is cold and rigid. To explain such a “cold corner”, the movement of slab and mantle need to be decoupled down to a certain depth by a thin, low viscosity layer (LVL) just above the slab so that hot material does not reach the corner of the mantle wedge. Many numerical studies have investigated the effects of slab-mantle coupling so far, although very few of them focus on its along-arc change. In this presentation, I will show how LVL at the plate interface affects the along-arc change in the degree of slab-mantle coupling.

I construct 3D finite element models to investigate a possible role of LVL in the subduction zone. The model domain is divided into crust, slab, and mantle wedge that includes LVL just above the slab. The flow is computed only in the mantle wedge and temperature is computed for the whole model domain. Buoyancy force is not considered and viscosity is assumed to be temperature and strain rate dependent except for LVL where it is constant. The model setting is exactly the same in the along-arc direction.

I find that when the viscosity of LVL is sufficiently low, the degree of slab-mantle coupling starts to change in the along-arc direction at some point and 3D flow and thermal structure develop. Temperature dependence of viscosity may be a key factor in producing such a feature. I also find that a thicker LVL leads to a longer wavelength of the 3D flow, and a deeper down-dip limit of LVL leads to a delayed onset of the 3D flow. In order to explain the spatial distribution of Quaternary volcanoes in Northeast Japan with this model, the viscosity and thickness of LVL need to be $<5\times10^{18}$ Pa.s and ~6 km, respectively. These results show that a detailed understanding of LVL including its formation process and spatial extent is essential to constrain the thermal structure in the subduction zone.

Keywords: subduction zone, slab-mantle coupling, distribution of volcanoes

Characteristics of slab-derived fluids beneath Kii Peninsula inferred from seismic traveltime tomography (2)

*Takuo Shibutani[1], Kazuro Hirahara[1]

1.Kyoto Univ.

1. Introduction
In order to investigate behavior and nature of slab-derived fluids discharged from the Philippine Sea plate subducting beneath Kii Peninsula, we have carried out seismic observations, receiver function analyses and seismic travel time tomography mentioned below. We estimated the geometry of the slab and the seismic velocity structure beneath the Kii Peninsula, and discussed the behavior of the fluids with the distribution of low velocity anomalies. We are now understanding relations between the fluids and deep low frequency events (DLFEs) and active micro seismicity beneath the northern Wakayama Prefecture.
2. Previous results
We carried out linear array seismic observations in the Kii Peninsula from 2004 to 2013. We deployed seismometers along profile lines with an average spacing of ~ 5 km. We applied a receiver function analysis and obtained images of S wave velocity discontinuities. We estimated 3D configurations of the continental Moho, the slab top and the oceanic Moho from receiver function images for four profile lines in the NNW-SSE direction which is the dip direction of the Philippine Sea plate and for two profile lines in the NNW-SSE direction that is almost perpendicular to the dip direction. A new knowledge obtained by the analysis is that the continental Moho dips upward in the southeast direction above the Philippine Sea slab.
We carried out the tomography with FMTOMO (Rawlinson et al., 2006) in which a robust wavefront tracking (de Kool et al., 2006) is implemented for the theoretical travel time calculation and the ray tracing. We used a velocity model with the 3D geometries of the three discontinuities derived from the receiver function analysis. We also used observed travel times at temporary stations in the dense linear arrays in addition to permanent stations. A dense distribution of the temporary stations contributed to higher resolutions of tomographic images. By analyzing travel time data for 74 months from May 2004 to the middle of 2010 we found that (1) DLFE areas show low velocity anomaly of ~5 % and (2) another strong low velocity anomaly (> 10 %) is widely distributed in the lower crust beneath the northern Wakayama Prefecture.
3. New attempts
Automatic picking of P and S times was carried out for the remaining waveform data in and after 2010. Travel time data for 33 months were added. They almost doubled the numbers of earthquakes and travel times utilized in the tomography. The result showed the similar features to (1) and (2) above. The result of checkerboard tests was improved in 22 -34 km depths. (1) can be due to discharged H_2O from hydrous minerals in the oceanic crust at 30 -40 km depths. (2) can be explained by a mechanism that fluids upwelling from the low velocity anomaly in the lower crust increase the pore pressure in existing cracks in the brittle upper crust. The Vp/Vs ratio of the low velocity anomaly beneath the northern Wakayama Prefecture has small values near 1.6. This might be due to silica-saturated fluids (Manning, 1996). The Vp/Vs ratio in the DLFE areas should be re-examined. We will contrive ways to estimate the Vp/Vs ratio by referring to Ramachandran and Hyndman (2012, Solid Earth).
We used waveform data from permanent stations of NIED; JMA; ERI, Univ. of Tokyo; Nagoya Univ. and DPRI, Kyoto Univ.

Keywords: tomography, slab-derived fluids, Kii Peninsula

Experimental constraints on the serpentinization rate of fore-arc peridotites: implications for the welling condition of the "Arima-type" hydrothermal fluids

*Takayuki Nakatani[1], Michihiko Nakamura[1]

1.Division of Earth and Planetary Materials Science Department of Earth Science Graduate School of Science, TOHOKU Univ.

In order to palce a constraint on the water circulation in subduction zones, hydration rates of peridotites have been investigated experimentally in fore-arc mantle conditions. Experiments were conducted at 400–580°C and 1.3 and 1.8 GPa, where antigorite was expected to form as a stable serpentine phase. Crushed powders of olivine ±orthopyroxene and orthopyroxene + clinopyroxene were reacted with 15 wt% distilled water for 4–19 days. The synthesized serpentine was lizardite in all experimental conditions except that of 1.8 GPa and 580°C in the olivine + orthopyroxene system, in which antigorite was formed. In the olivine + orthopyroxene system, the reactions were interface-controlled except for the reaction at 400°C, which was diffusion-controlled. Corresponding reaction rates were 7.0 $\times10^{-12}$–1.5 $\times10^{-11}$ $m\cdot s^{-1}$ at 500–580°C and 7.5 $\times10^{-16}$ $m^2\cdot s^{-1}$ at 400°C for the interface- and diffusion-controlled reactions, respectively. Based on a simple reaction-transport model with these hydration rates, we infer that leakage of the slab-derived fluid from an water-unsaturated fore-arc mantle is allowed only when focused flow occurs with a spacing larger than 77–229 km in hot subduction zones like Nankai and Cascadia, whereas the necessary spacing is just 2.3–4.6 m in intermediate-temperature subduction zones like Kyushu and Costa Rica. These calculations suggest that fluid leakage in hot subduction zones may occur after the fore-arc mantle is totally hydrated, while in intermediate-temperature subduction zones, leakage through a water-unsaturated fore-arc mantle may be facilitated.

Keywords: hydration reaction, slab-fluid, serpentine, fore-arc mantle

Feedback among reaction, mass transport and fracturing during metamorphism: controls and and pattern formation

*Atsushi Okamoto[1], Hiroyuki Shimizu[2]

1.Graduate School of Environmental Studies, Tohoku Univ., 2.Institute of Fluid Science, Tohoku Univ.

Analyses of equilibrium phase relations with recently-developed thermodynamic dataset of rock-forming minerals has provided us significant information on distributions of stable mineral assemblage and water content within the Earth’s interiors. However, based on the petrological observations of metamorphic rocks and serpentinites, thermodynamic equilibrium is not always attained during metamorphism at individual P-T conditions, and unreacted parts often remain. To understand the dynamic behavior of the Earth’s interior, it is important to investigate essential controls on the progress of metamorphic reactions. We have developed a novel model for the coupled processes of surface reaction, fluid transport and fracturing during metamorphic reactions by a distinct element method (DEM) (Okamoto and Shimizu, 2015). This model considers a reaction rate as a function of fluid pressure, and revealed that contrasting fracture patterns are produced between volume-decreasing dehydration (typical in prograde metamorphism) and volume-increasing hydration reactions (retrograde metamorphism, or serpentinization).
In this contribution, we focus on the relative rate of fluid transport and surface reaction on the fracture pattern during the volume-increasing hydration reaction. The new DEM model treats transport of water in two ways; flow along the fractures and flow through matrix. The latter has the similar effects to diffusion. For evaluate the system, we introduce two nondimensional parameters; the ratios of the rates of fracture flow (Y_F) and diffusion (Y_D) to the surface reaction rate. We found systematic changes in fracture pattern and system evolution as a function of Y_D and Y_F. In the first case that reaction is faster than water transports (Y_D <1 and low Y_F <1), the reaction proceeds from the boundaries and forms fine fractures layer-by-layer. In the second case that reaction is faster than diffusive transport of water but much slower than flow along the fracture (low Y_D<1 and high Y_F >1000), the reaction proceeds inward effectively to form hierarchical fracture networks. In the third case with high diffusion rate (Y_D >10), the reaction tends to proceed from the boundaries without fracturing. The dependence of the fracture pattern on Y_F and Y_D suggests the importance of the rates of water transport relative to the surface reaction rate in studying the mechanism and overall rate of water–rock reactions. The fracture pattern generated in the second case is similar to mesh texture found in the partly serpentinized peridotite in oceanic peridotites. We also discuss the effects of grain boundaries and will develop the model to more realistic reaction system which incorporate element diffusion such as silica.

Okamoto and Shimizu (2015) Earth Planet Sci Let, 417, 9-18.

Keywords: reaction-transport-fracturing feedback, distinct element method, serpentinization

Influence of pore size distribution on elastic wave velocities during evaporative drying

*Takuya Horikawa[1], Tadashi Yokoyama[1]

1.Department of Earth and Space Science, Graduate School of Science, Osaka University

Elastic wave velocities (V_P,V_S) in porous rocks are known to be sensitive to the water saturation (S), the size and shape of pores, the distribution of fluids in pores, and the incident wave frequency. Various studies have tried to understand these dependences on the basis of Biot’s theory (Biot, 1956). The method for accurately predicting the quantitative relationship between S and V_P, V_S for the entire range of S (from S = 1 (saturated) to S = 0 (dry)) still remains to be fully elucidated. In this study, we measured the changes of V_P and V_S during drying for two Berea sandstones (permeabilities: 300 mD, 20 mD; hereafter described as Berea300 and Berea20, respectively) and Shirahama sandstone (permeability: <0.6 mD). P-wave and S-wave frequencies used in the measurements were 200 kHz and 100 kHz, respectively. The measured pore size distributions (aperture radius) showed that the predominant pore radii were ~5-100 μm for Berea300, ~1-10 μm for Berea20, and less than 0.4 μm for Shirahama. The change of V_P with S for Berea300 can be classified into the following 4 stages: [(1) S=1→0.5: decrease of V_P; (2) S=0.5→0.3: increase of V_P; (3) S=0.3→0.1: decrease of V_P; (4) S=0.1→0: increase of V_P]. The change of V_S with S for Berea300 can be separated to 2 stages: [(1) S=1→0.15: gradual increase of V_S; (2) S=0.15→0: rapid increase of V_S]. For Berea20, the V_P change trend appeared to correspond to part of stage 1 plus the entire range of stages 2, 3, 4 observed in Berea300, and the V_S change trend was approximately equal to that in Berea300. For Sirahama, the V_p change trend seemed to be equivalent to the stages 3 and 4 in Berea300, whereas V_S decreased first and then increased, unlike in the case of Berea sandstones. When the drying proceeds, it is known that water is lost first in the larger pores, and later in the smaller ones (Nishiyama et al., 2012). Therefore, the size of pores containing water at a given S can be determined on the basis of the pore size distribution of each rock. By incorporating the information of pore size distribution and the frequency dependence of bulk modulus into previously reported models, we tried to precisely predict the change of V_P and V_S during drying.

Keywords: Elastic wave, Water saturation, Pore size distribution, Sandstone

Effect of pore fluid on seismic velocity of serpentinite and the origin of high Vp/Vs in mantle wedge

*Ikuo Katayama[1], Yunxi Liu[1], Kanta Zaima[1]

1.Department of Earth and Planetary Systems Science, Hiroshima University

Serpentine is one of the candidates to explain low-velocity anomaly and high Vp/Vs in mantle wedge. However, extremely high Vp/Vs found beneath Kanto and southwest Japan requires the presence of aqueous fluid in addition to the serpentinites. In this study, we investigated the effect of pore fluid on elastic-wave velocity of antigorite during triaxial deformation using intra-vessel apparatus at Pc = 10-20 MPa, Pp = 5-10 MPa and room temperature. Compressional and shear-wave velocities decrease during deformation, possibly due to the formation of micro-cracks in the specimen. Since shea-wave velocity changes more drastically than compressional-wave velocity, Vp/Vs increases during deformation, which is consistent with the crack model by O’Connel and Budiansky (1974). In future, we are going to monitor volume change of pore fluid during deformation, and discuss the amounts of pore fluid to explain the observation of high Vp/Vs in mantle wedge.

Keywords: serpentinite, seismic velocity, pore fluid

Elastic constants of single-crystal topaz and their temperature dependence studied via sphere-resonance method

*Fumie Sema[1], Tohru Watanabe[1]

1.Graduate School of Science and Engineering, University of Toyama

Transport of ocean floor sediments by plate motions might play an important role in the circulation of materials within the Earth. Imaging subducted sediments through seismological observations requires a thorough understanding of elastic properties of sediment origin hydrous minerals. Topaz is a hydrous mineral, which can be formed from subducted sediment at high pressures. We have studied elastic constants of single-crystal topaz and their temperature dependence by the sphere-resonance method.
A sphere sample (D=6.483(1) mm) was made from a topaz single-crystal ($Al_{1.97}SiO_4(F_{1.56},OH_{0.42})$) collected from Nakatsugawa, Gifu Pref. by the two-pipe method. The uniformity of crystallographic orientation was confirmed with SEM-EBSD (Shizuoka Univ.) measurement. Resonant frequencies were measured at frequencies from 600 kHz to 1.5 MHz with different specimen-holding forces. Extrapolating to the specimen-holding force of zero, we obtained frequencies of "free" oscillation. The temperature was changed from 0 to 40ºC. Elastic constants were determined by comparing measured and calculated resonant frequencies. The xyz algorithm (Visscher et al., 1991) was employed to calculate resonant frequencies of the sphere sample. At room temperature (18.7ºC), C11=281.3, C22=346.3, C33=294.8, C44=108.5, C55=132.5, C66=130.3, C12=121.5, C13=80.90, C23=81.73 (GPa). Using determined elastic constants, compressional- and shear-wave velocities were estimated for an isotropic polycrystalline aggregate of topaz at high temperature. Compresional- and shear-wave velocities at 800ºC are 9.32 km/s and 5.57 km/s, respectively. These values are significantly higher than those in minerals like olivine or garnet.

Keywords: elastic constants, resonance method, hydrous mineral, topaz

A new mechanism to produce chemical heterogeneity of Earth's mantle: Slab dehydration at 660-km phase boundary

*Atsushi Nakao[1,2], Hikaru Iwamori[1,2], Tomoeki Nakakuki[3]

1.Department of Earth and Planetary Sciences, Tokyo Institute of Technology, 2.Department of Solid Earth Geochemistry, Japan Agency for Marine-Earth Science and Technology, 3.Department of Earth and Planetary Systems Science, Hiroshima University

Introduction

Dehydration-hydration processes are thought to be essential for creating chemical heterogeneity in the Earth's mantle: e.g., the mantle geochemical end-member "HIMU" likely represents recycling of an extremely dehydrated oceanic crust, and mantle geochemical hemispheres (Iwamori and Nakamura, 2012) seem to be originated from dehydration-hydration reactions in subduction zones. We investigate behaviors of hydrophilic components during mantle convection and water transport using a self-consistent numerical model in order to reveal the chemical evolution of Earth's mantle with geophysical validity.

Methods

A 2-D fluid mechanical simulation with following characteristics is conducted.
(1) Free convection of whole-mantle scale without synthetic forces (Tagawa et al., 2007).
(2) Phase diagrams of hydrous peridotite and hydrous basalt (Iwamori, 2007) to introduce hydration and dehydration reactions.
(3) Realistic constitutive and state equations for the hydrous rocks to make (1) and (2) interactive.
(4) Transport of multiple elements that can be partitioned between mantle rocks and aqueous fluid using a Marker-in-Cell technique.

Results and Discussion

During slab subduction, dehydration reactions occur at specific p-T conditions. Then instantaneous aqueous fluid enriched in hydrophilic components and less-hydrated residue minerals depleted in the components are produced. The aqueous fluid is assumed to be immediately incorporated into dry rocks through which the fluid percolates. The transported hydrophile elements are assumed to precipitate with the fluid. In each run, three major dehydration and fractionation processes are reproduced as follows.

[Process 1] (Depth < 200 km; under-arc process) Associated with dehydration of the subducted slab, discharge of highly hydrophilic elements results in depletion of the slab subducting into deeper mantle. The hydrophilic elements are deposited into the overlying lithosphere. This process does not contribute to global redistribution of hydrophile elements, because of high viscosity in the cold region. The depleted layer is fixed along the subducting slab for a long time.

[Process 2] (Depth = 660 km; slab penetration process) When the slab penetrates into the lower mantle, the hydrophiles are continuously emitted depending on their partition coefficients during dehydration associated with wet-Rw →Pv + MgO + Aq transition. This process helps heterogeneity in terms of the hydrophile elements to horizontally expand. During the slab penetration process, the depleted rock as a product of 660-km dehydration is produced just below the phase boundary, and descends into the deeper mantle.

[Process 3] (Depth = 410 km; upwelling wet plume process) If the water-saturated layer is formed just above the 660-km phase boundary, wet plumes enriched in the hydrophiles ascend due to their buoyancy. After plumes reach the 410-km phase boundary, dehydration by Wd →Ol transition and the corresponding fractionation of the hydrophiles occur. However, the depleted plume tails are not

well separated from the enriched plume head.
Among them, [Process 2] is the most efficient process for creating and distributing the geochemical heterogeneity. [Process 2] with wet plumes and aqueous porous flows from the 660-km phase boundary involves a possible mechanism to produce the observed geochemical hemispheres representing a hydrophile-rich part (eastern hemisphere) and a depleted part (western hemisphere) (Iwamori and Nakamura, 2012).

Keywords: hydrophilic trace elements, water transportation, mantle convection, 660-km phase boundary, chemical heterogeneity of mantle, element partition

Iron-titanium oxyhydroxides as a water transporter into the Earth's mantle transition zone

*Kyoko N. Matsukage[1], Yu Nishihara[2], Xingcheng Liu[1], Toshihiro Suzuki[1], Yusuke Seto[3], Eiichi Takahashi[1]

1.Earth and Planetary Sciences, Tokyo Institute of Technology, 2.Geodynamics Research Center, Ehime University, 3.Department of Planetology, Kobe University

We experimentally discovered a new hydrous phases, iron-titanium oxyhydroxides, in the system basalt + H_2O at pressure of 12 GPa and temperature of 1000°C which corresponds to condition of the deep upper mantle in the slab (Matsukage et al. submitted). These new hydrous phases have chemical compositions in the system FeOOH-TiO_2. However, their small grain sizes in basalt + H_2O system has hindered efforts to determine their crystal structures and to confirm the presence of water.
We synthesized single phase in the system FeOOH-TiO_2 at pressures of 8-16 GPa and temperatures of 900–1600°C which corresponds to conditions of the deep upper mantle and the mantle transition zone (Nishihara and Matsukage, 2016). Seven different compositions in the FeOOH-TiO_2 system having molar ratios of x = Ti/(Fe + Ti) = 0, 0.125, 0.25, 0.375, 0.5, 0.75 were used as starting materials. High-pressure and high-temperature experiments were carried out using Kawai-type multi-anvil apparatus (Orange-1000 at Ehime University, SPI-1000 and SAKURA at Tokyo Institute of Technology). In this system, we identified two stable iron-titanium oxyhydroxide phases whose estimated composition is expressed by $(FeH)_{1-x}Ti_xO_2$. One is the Fe-rich solid solution (x < 0.23) with e-FeOOH type crystal structure (e-phase, orthorhombic, $P2_1nm$) that was described by the previous studies (e.g., Suzuki 2010), and the other is the more Ti-rich solid solution (x > 0.35) with a-PbO_2 type structure (a-phase, orthorhombic, *Pbcn*). The a-phase is stable up to 1500ºC for a composition of x = 0.5 and at least to 1600ºC for x = 0.75. Our result means that this phase is stable at average mantle temperature in the Earth's mantle transition zone.
We also found that the hydrous phase with a-PbO_2 type structure was stable in basalt + H_2O system at wide pressure range at deep upper mantle and mantle transition zone (8-17 GPa), and it dehydrate at pressure of ~17 GPa. Above 17 GPa, CaTi perovskite was formed as a Ti-bearing phase. After dehydration of FeTi oxyhydroxide, Al-bearing phase D, which is one of major water carriers in deep mantle, was stable (Liu et al., this meeting). Therefore our findings suggest that water transport in the Earth's deep interior by basaltic crust is probably much more efficient than had been previously thought.

Keywords: deep upper mantle, mantle transition zone, water, titanium, hydrous phase, basaltic crust

Prediction of elemental partition between fluid and melt by bond valence method

*Masami Kanzaki[1]

1.Institute for Study of the Earth's Interior, Okayama University

Matsui, Onuma and others (Bull. Soc. fr. Mineral. Crystallogr., 1977) revealed that elemental partition between minerals and magma is mostly governed by local structure of ion sites in crystalline phases, and accordingly elemental partition has been predicted by Nagasawa model or similar models. However, these models can not be applied to partition between fluid and melt, as these models do not explicitly treat these phases. Recently, the author found that “bond valence” method can be applied to predict partition behavior. Initial tests to crystalline phases are promising. So, I’m currently trying to extend this method to fluid and melt.

Bond valence method is an extension of Pauling’s original idea, that valence of central cation can be divided into each bond in ionic crystals. I.D. Brown extended this by including bond distance dependence to bond valence; longer bond has lower bond valence. In ionic crystals, bond valence sum on central atom coincides with its valence or very close to it. If deviation is large, something wrong with the structure. To date, several authors compiled bond valence parameters using databases of crystal structures for almost all elements except rare gases. Therefore, if crystal structure (or at least local structure) is known, bond valence sum (bvsum) can be calculated. For example, if we put Sr in M2 site of forsterite, we will have bvsum larger than 2, as Sr ion is too large for M2 site. This difference is related to "strain" energy, as bond valence equation ($\exp((R_0-r_{ij})/B)$) is identical to repulsive term of two-body inter-ionic potentials. So, I defined misfit parameter; misfit = abs(bvsum - Q) where Q is valence of central cation. If we take difference of misfits between two distinct crystallographic sites (e.g., M1 and M2 sites of forsterite), it can be related to partition coefficient. In this way, “partition coefficient” of intra- and inter-crystalline phases are calculated, and they can compare well with experimental data. This calculation is very simple, and only bond distances and bond valence parameters are necessary. Prediction of partition behavior such as perovskite/postperovskite is now possible. It was found that bond valence method can be used to quantitatively predict elemental partition, however, there are several unsolved issues, such as how to quantitatively relate difference of misfits to partition coefficients, and how to treat different valences consistently etc.

If we know the local structures of fluid and melt, partition behavior can be qualitatively predicted using present method. However, this is not the case at moment. Therefore, single virtual site for each fluid and melt was assumed, then partition behavior between two sites was evaluated by changing size of the sites. Based on Pearce et al. (doi:10.1029/2004GC000895), Ba, Cs, K, Pb and Sr prefer fluid, whereas REE, Nb, Ta, Zr, Hf etc. prefer melt. Such behavior was reproduced when the size of the site for fluid is about 3.2 A, and that of melt is 2.5 A. Using this local structure model, partition behaviors of other elements can be predicted. Alternatively, local structures of fluid and melt could be estimated by comparing precisely determined partition data with present model.

Keywords: bond valence method, elemental partition, fluid, melt, local structure

Is the non-destructive analysis of carbon isotope ratio useful?

*Kohei Takahata[1], Junji Torimoto[2], Junji Yamamoto[3]

1.Earth and Planetary System Sciences, Hokkaido University, 2.JAMSTEC, 3.Hokkaido University Museum

Carbon is an important volatile element that has had a great influence on the environment of the Earth's surface through the history. Carbon dioxide has a greenhouse effect gas and this gas exhausted by our production activities is regarded as a cause of modern global warming.
Carbon dioxide is observed as the fluid inclusions in the mantle xenolith that is derived from deep earth. A paper reports that the integral exhaust amount of carbon from the deep earth is equal to the amount of the carbon that exists on the Earth's surface in present. Therefore it is important for the discussion of environmental issues to understand the origin of the deep earth carbon and the cycle of carbon using mantle xenolith.
The modern sampling method of carbon dioxide fluids (Crushing method) has two problems, the destruction of the samples and the shortage of the spatial resolution. The measurement of carbon isotope ratio using Raman spectroscopy has a possibility to break through those problems. However, this method hasn't had the precision to be able to discuss the origin of carbon dioxide fluids yet. In this study, we tried to improve the precision of the measurement of carbon isotope ratio using Raman spectroscopy using a micro-Raman spectrometer with high spectral resolution. Moreover, we discuss the cause of uncertainty depends on the result of measurement and the prospects for the future.
As a result of measurement, the uncertainty of this method is revealed ±26‰ (1 σ) at 1500 sec. A reason of this bad uncertainty is the shortage of sensitivity of the Raman spectrometer. The lowness of signal noise ratio (S/N) with the low sensitivity causes a lack of precision of the peak fitting. We can estimate the ultimate precision of this method by assuming an infinite peak count using regression line. For the analytical system of this study, the limit value is ±11‰ (1 σ), which is still worse than the precision to be able to discuss the origin of carbon in mantle xenolith.
The factor of this error is revealed the apparent Raman shift depends on the changing of room temperature. If it does not exist, the precision can improve to discuss the origin of deep carbon.

Keywords: carbon dioxide, fluid inclusion, Raman spectroscopy, mantle xenolith, carbon isotope ratio

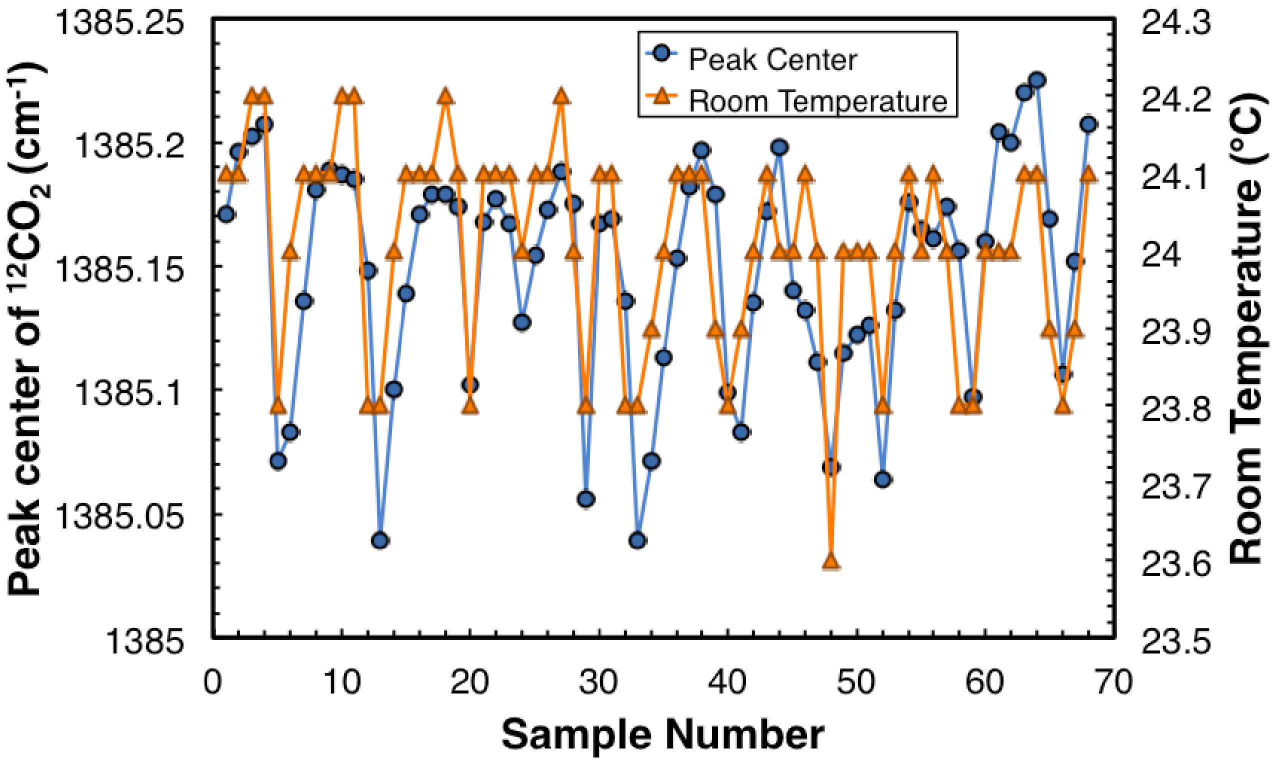

Peak center of $^{12}CO_2$ (cm^{-1})
1385.25
1385.2
1385.15
1385.1
1385.05
1385
Peak Center
Room Temperature
Room Temperature (°C)
24.3
24.2
24.1
24
23.9
23.8
23.7
23.6
23.5
0
10
20
30
40
50
60
70
Sample Number